Journal of
Nanoscience and Nanotechnology
Vol. 13, 1765–1768, 2013

Amorphous Carbon Nanotube/MnO_2/Graphene Oxide Ternary Composite Electrodes for Electrochemical Capacitors

Changbin Im, Young Soo Yun, Bona Kim, Hyun Ho Park, and Hyoung-Joon Jin*

Department of Polymer Science and Engineering, Inha University, Incheon 402-751, Republic of Korea

Ternary composites of amorphous carbon nanotube/MnO_2/graphene oxide (*a*-CNT/MnO_2/GO) were synthesized by a facile direct redox reaction between potassium permanganate and *a*-CNT, which was prepared by anodic aluminum oxide template method following co-filtration with GO. Needle-like, 100-nm-thick, MnO_2 crystals were homogeneously coated on the *a*-CNT surface, which was then covered with GO. The electrochemical performance of the resulting MnO_2-coated *a*-CNTs exhibited a specific capacitance of 473 F/g at a scan rate of 5 mV/s, and excellent charge/discharge stability after 500 cycles.

Keywords: Graphene, Manganese Oxide, Graphene Oxide, Supercapacitor, Pseudocapacitance.

1. INTRODUCTION

Electrochemical capacitors (ECs) have attracted considerable attention as an alternative energy storage/conversion device due to their higher power density, faster charge/discharge rates and longer cycle life than common batteries.[1–2] Manganese oxide (MnO_2) has drawn much attention as a charge storage material for ECs owing to its low cost, natural abundance, environmental compatibility, and high theoretical specific capacitance (1370 F/g). However, its poor electronic conductivity, relatively low cycle ability, and dense morphology are barriers to high capacitance.[3] In order to overcome these problems, many studies related to MnO_2 composites with carbonaceous materials have been reported in terms of high specific capacitance, and rate capability with high surface area and electronic conductivity. The composite system was mainly applied to a binary system composed of carbon materials and MnO_2 and enhanced their electrochemical performance.[4] Graphene, a two-dimensional carbon material, has unique physical, chemical, and electrical properties.[5]

Graphene oxide (GO) is easily available through the controlled chemical oxidation of graphite. GO contains oxidation regions such as the epoxide, hydroxyl groups and carboxyl groups. The presence of these functional groups makes GO strongly hydrophilic, which allows GO to readily swell and disperse in water.[6–7] In this study, we prepared *a*-CNTs/MnO_2/GO ternary composite electrodes for ECs. The *a*-CNTs were coated with MnO_2 and then covered with GO. The ternary composite electrodes exhibited high specific capacitance and good cycle stability.

2. EXPERIMENTAL DETAILS

2.1. Preparation of *a*-CNTs

Poly(vinylpyrrolidone) (MW ≈ 55,000 g/mol) was dissolved in dichloromethane (20 ml) and impregnated directly into the pores of the alumina template by wetting method.[8] After complete solvent evaporation, the membrane was carbonized at 700 °C under N_2 atmosphere. After 2 h of carbonization, the carbonized membrane was cooled to room temperature. The carbonized membrane was then immersed in 48% HF at room temperature for 24 h to remove the alumina template. The product was then washed with distilled water to remove the residual HF and was dried at 80 °C to obtain *a*-CNTs powders.

2.2. Preparation of *a*-CNTs/MnO_2/GO Ternary Composites

MnO_2 was spontaneously deposited onto the synthesized *a*-CNTs by a direct redox reaction between the *a*-CNTs and MnO^{4-}. Then 0.1 g of the synthesized *a*-CNTs was added to 200 ml of 0.1 M $KMnO_4$. The pH of the solution

*Author to whom correspondence should be addressed.

RESEARCH ARTICLE

was adjusted by using 0.01 M HCl. The reaction temperature was maintained at 70 °C with vigorous stirring. The *a*-CNTs/MnO_2 binary composite was washed with distilled water to remove unreacted MnO^{4-} and dried in an oven at 80 °C. GO was prepared using Hummer's method. Then, 0.1 g of the *a*-CNT/MnO_2 composite was mixed with 0.05 g of GO in ethanol. After sonication for 1 h, the *a*-CNTs/MnO_2/GO solution was filtered and completely dried in an oven. For strong binding between the composite materials, the final annealing process was conducted at 200 °C under a N_2 flow of 200 ml/min for 2 h.

2.3. Characterization

The morphology of the synthesized composites was characterized by field emission scanning electron microscopy (FESEM, S-4300, Hitachi, Japan), transmission electron microscopy (TEM, CM200, Philips, U.S.A.) and atomic force microscopy (AFM, Digital Instrument Nanoscope IVA). The crystal phase structure of the composites was determined by detecting the peaks of the MnO_2 using X-ray diffraction (XRD, DMAX-2500, Rigaku, Japan) by means of a diffractometer with reflection geometry and CuKα radiation (wavelength $\lambda = 0.154$ nm) operated at 40 kV and 100 mA. X-ray photoelectron spectroscopy (XPS, AXIS-HIS, Kratos Analytical, Japan) was employed with a dual-chromatic MgKα X-ray source at 1500 eV. The working electrode was prepared via the following steps. The as-prepared composite and poly (tetrafluoroethylene) were mixed in a mass ratio of 9:1 without additional conductive materials and dispersed in ethanol. The resulting slurry was coated onto the nickel substrate (0.2826 cm^2) with a spatula. Next, nickel foam with the composite slurry was dried at 110 °C in a vacuum oven for 12 h. All electrochemical measurements were carried out in a three-electrode cell connected to an electrochemical analyzer (AutoLab PGSTAT12, Eco Chemie). The nickel mesh containing the electroactive materials, platinum plate and saturated KCl were used as the working, counter and reference electrodes, respectively. Cyclic voltammetry (CV) tests were carried out over a range of 0 to 1.0 V at different scan rates of 5, 10, 20, and 50 mV/s.

3. RESULTS AND DISCUSSION

We successfully fabricated *a*-CNTs using anodic aluminum oxide template method and carbonization. The length of the *a*-CNTs ranged from 5~10 μm, and their average diameter was about 200 nm with a wall thickness of a few nanometers. Figures 1(A) and 1(B) show the TEM images of the MnO_2-coated *a*-CNTs. The MnO_2-loading contents were dependent on the immersion time of the *a*-CNTs in $KMnO_4$ solution. In spite of the harsh oxidation process of *a*-CNTs, the original CNT morphology, such as a diameter of 200 nm, was well preserved and

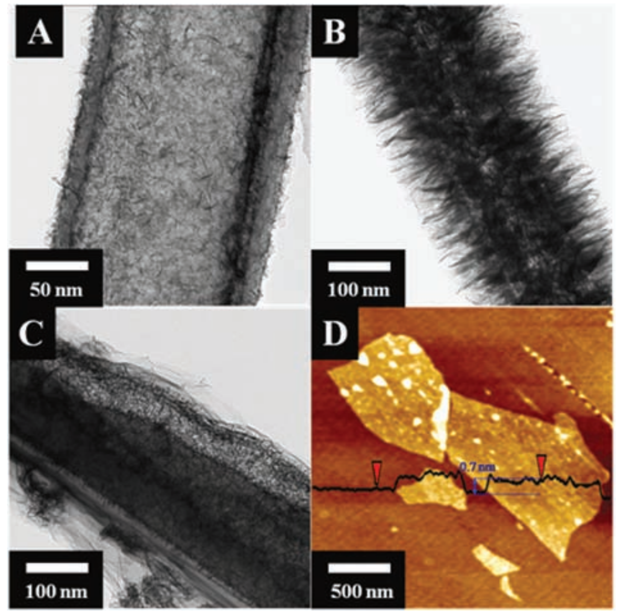

Fig. 1. SEM image of MnO_2-coated *a*-CNT with immersion times of (A) 1 h and (B) 4 h, and (C) *a*-CNT/MnO_2 composite covered by GO. (D) AFM image of GO.

needle-like MnO_2 crystals were coated on the *a*-CNTs by controlling the loading time.

The MnO_2-coated *a*-CNTs were dispersed in GO dispersion, in which GO, with a sub-nanometer thickness and lateral size of several hundred nanometers (Fig. 1(D)), was dispersed in ethanol. The mixture solution was then vacuum-filtered. As a result, the *a*-CNT/MnO_2 composite was covered by GO (Fig. 1(C)).

Details of the *a*-CNTs/MnO_2/GO ternary composite fabrication process are depicted in Figure 2. In step A, the *a*-CNTs were fabricated by the anodic aluminum oxide template method and carbonization. Step B shows the MnO_2 deposition process on the synthesized *a*-CNTs. MnO_2 was formed by the reduction of MnO^{4-} ions on the surface of the *a*-CNTs. The reduced MnO_2 on the surface of the *a*-CNTs was mixed with GO fabricated via step C and then the products were filtered and annealed at 200 °C in Step D.

Figure 3(A) shows the XRD patterns of the *a*-CNTs, *a*-CNTs/MnO_2 binary composite, *a*-CNTs/MnO_2/GO ternary composite and α-MnO_2. The *a*-CNTs exhibited a sharp peak at around 26° and a broad weak peak at around 44°, which are characteristic of graphitic carbon. In the *a*-CNT/MnO_2 binary composite, the three major diffraction peaks of 2θ at around 12°, 37° and 66° were assigned to the crystal planes of (1 1 0), (2 1 1) and (0 0 2) in α-type MnO_2 (JCPDS 44-0141), respectively. The crystal structure of the *a*-CNTs/MnO_2/GO ternary composite revealed that the α-MnO_2 structures disappeared and the graphitic carbon peaks were broadened. This suggests that the *a*-CNT/MnO_2 binary composites were amorphous.

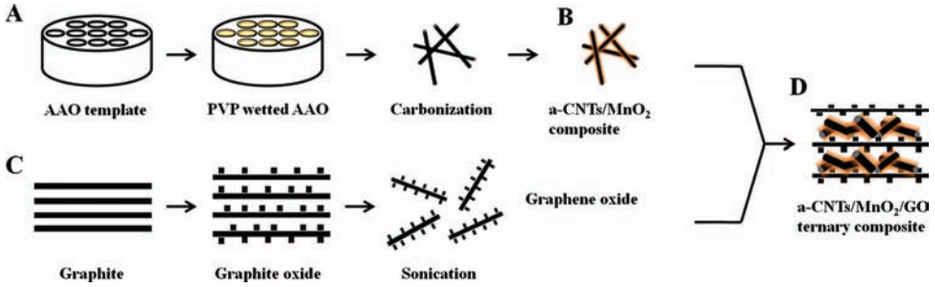

Fig. 2. Schematic diagrams of the preparation process of the *a*-CNTs/MnO_2/GO ternary composite.

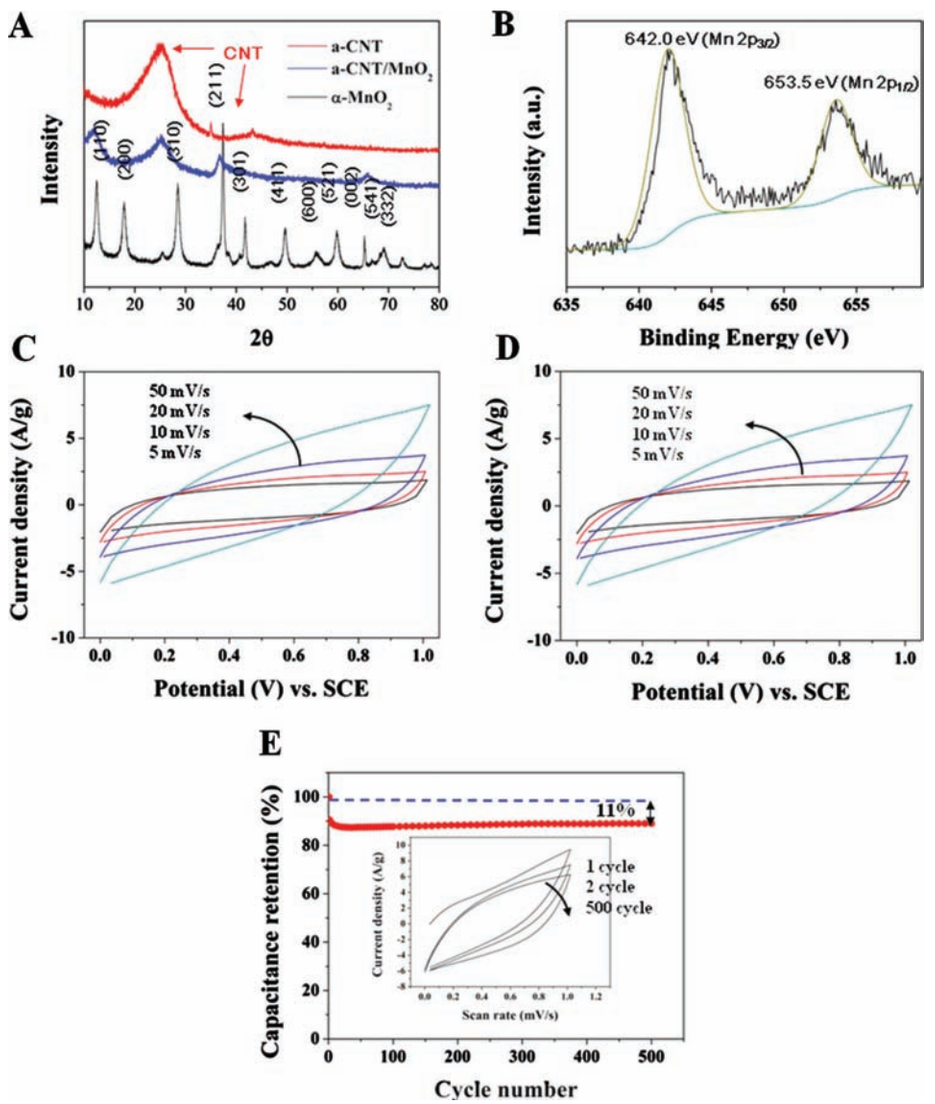

Fig. 3. (A) XRD patterns of the *a*-CNTs (red), *a*-CNTs/MnO_2 binary composite (blue), *a*-CNTs/MnO_2/GO ternary composite (green) and α-MnO_2 (black). (B) XPS spectra of the Mn 2p region of the *a*-CNT/MnO_2/GO ternary composites. (C) Cyclic voltammograms at different scan rates (black-5 mV/s, red-10 mV/s, blue-20 mV/s and cyan-50 mV/s). (D) Cyclic voltammograms of α-MnO_2, *a*-CNT/MnO_2 binary composites and *a*-CNTs/MnO_2/GO ternary composite electrodes at a scan rate at 5 mV/s. (E) Variations of the specific capacitance of the *a*-CNTs/MnO_2/GO ternary composite electrode as a function of cycle number at 50 mV/s.

RESEARCH ARTICLE

The amorphous regions can increase the specific capacitance of supercapacitors because the amorphous structure can aid the insertion and deinsertion of the electrolyte from the oxide surface, which can increase the contact between the electrolyte and the electrode material, and consequently improve the efficiency of the electrode.

The surface information of the *a*-CNTs/MnO_2/GO composites was collected by XPS. The binding energies revealed the presence of MnO_2 with the *a*-CNTs. The Mn $2p_{3/2}$ peak was centered at 642.0 eV and the Mn $2p_{1/2}$ peak at 653.5 eV, with a spin-energy separation of 11.7 eV in Figure 3(B). These results agreed well with the reported data of Mn $2p_{3/2}$ and Mn $2p_{1/2}$ in MnO_2.[9] They were also consistent with the aforementioned XRD analysis.

The electrochemical behavior of the *a*-CNT/MnO_2/GO ternary composites was analyzed in 1 M Na_2SO_4 aqueous solution. Figure 3(C) shows the CV curves of the *a*-CNT/MnO_2/GO ternary composite electrodes at scan rates of 5, 10, 20 and 50 mV/s. At all scan rates, the CV curves exhibited symmetrical and rectangular-like shapes, which indicated an ideal capacitive behavior. The specific capacitances of the ternary composite electrodes were 473, 307, 221, and 150 F/g at scan rates of 5, 10, 20 and 50 mV/s, respectively. The pseudocapacitance of MnO_2 in aqueous electrolytes has previously been attributed to the following redox reaction in Eq. (1):

$$MnO_2 + \delta X^+ + \delta e^- \leftrightarrow MnOOX_\delta \quad (1)$$

where X^+ corresponds to H^+ or alkali metal cations such as Na^+ and K^+.[10] On the basis of Faraday's law, the theoretical specific capacitance of the reduction of Mn(IV)O_2 to Mn(III)OOX is approximately 1100 F/g with a voltage window of 1.0 V.[11]

However, the electrochemical performance MnO_2-only was poor (9 F/g). In the binary composite in which MnO_2 was deposited uniformly on the *a*-CNT surface, the specific capacitance was enhanced to 148 F/g. For the ternary composite, the GO layer covering the binary composite can act as both a supplement for electronic conductivity and a barrier to the falling out of MnO_2. As a result, an improved specific capacitance of 473 F/g was demonstrated in Figure 4(D). Figure 4(E) shows the cycle stability according to the charge/discharge cycle number at a scan rate of 50 mV/s. The total decline of the specific capacitance was 11% of the initial capacitance (166 F/g to 150 F/g). Except for the 1st cycle, the electrode exhibited excellent cycle stability over the entire cycle numbers. After 500 cycles, the capacitance decreased by only 1.6% from the initial capacitance (150 F/g to 147.8 F/g), which was attributed to the GO layer covering the MnO_2 coating. Although the mechanism of capacitance degradation has not yet been elucidated, it is believed that carbonaceous materials of the composite improved the cyclic stability by reducing the stress.

4. CONCLUSION

Ternary composites of *a*-CNTs/MnO_2/GO, in which *a*-CNTs with high aspect ratio were coated by needle-like MnO_2 crystals and then covered with GO, were successfully synthesized and their electrochemical performance was investigated. The specific capacitances of the ternary composite electrodes reached 473 F/g and the composite also showed good cycle stability in that the specific capacitance only decreased by 2% between the 2nd and 500th cycles at a scan rate of 50 mV/s.

Acknowledgments: This work was financially supported by a grant from the Fundamental R&D Program for Core Technology of Materials funded by the Ministry of knowledge Economy, Republic of Korea.

References and Notes

1. P. Simon and Y. Gogotsi, *Nat. Mater.* 7, 845 (**2008**).
2. B. E. Conway, *J. Electrochem. Soc.* 138, 1539 (**1991**).
3. Z.-S. Wu, W. Ren, D.-W. Wang, F. Li, B. Liu, and H.-M. Cheng, *ACS Nano* 4, 5835 (**2010**).
4. Q. Li, J. Liu, J. Zou, A. Chunder, Y. Chen, and L. Zhai, *J. Power Sources* 196, 565 (**2011**).
5. Y. Zhu, S. Murali, W. Cai, X. Li, J. W. Suk, J. R. Potts, and R. S. Ruoff, *Adv. Mater.* 22, 3906 (**2010**).
6. Y. S. Yun, Y. H. Bae, D. H. Kim, J. Y. Lee, I.-J. Chin, and H.-J. Jin, *Carbon* 49, 3553 (**2011**).
7. Y. S. Yun, D. H. Kim, Y. Tak, and H.-J. Jin, *Synthetic Met.* 161, 2460 (**2011**).
8. J.-T. Chen, K. Shin, J. M. Leiston-Belanger, M. Zhang, and T. P. Russell, *Adv. Funct. Mater.* 16, 1476 (**2006**).
9. Q. Qu, P. Zhang, B. Wang, Y. Chen, S. Tian, Y. Wu, and R. Holze, *J. Phys. Chem. C* 113, 14020 (**2009**).
10. L. Benhaddad, L. Makhloufi, B. Messaoudi, K. Rahmouni, and H. Takenouti, *J. Mater. Technol.* 27, 585 (**2011**).
11. S.-B. Ma, K.-W. Nam, W.-S. Yoon, X.-Q. Yang, K.-Y. Ahn, K.-H. Oh, and K.-B. Kim, *J. Power Sources* 178, 483 (**2008**).

Received: 10 November 2011. Accepted: 22 February 2012.